

Investigating the synergistic potential Si and biochar to immobilize soil Ni in a contaminated calcareous soil after *Zea mays* L. cultivation

Hamid Reza Boostani¹, Ailsa G. Hardie², Mahdi Najafi-Ghiri¹, Ehsan Bijanzadeh³, Dariush Khalili⁴, Esmaeil Farrokhnejad¹

¹Department of Soil Science, College of agriculture and natural resources of Darab, Shiraz University, Darab74591, Iran.

²Department of Soil Science, Faculty of AgriSciences, Stellenbosch University, Private Bag X1, Matieland 7602, South Africa

³Department of agroecology, College of agriculture and natural resources of Darab, Shiraz University, Darab 74591, Iran

⁴Department of Chemistry, College of Sciences, Shiraz University, Shiraz 71454, Iran

Correspondence to: Hamid Reza Boostani (hr.boostani@shirazu.ac.ir)

Abstract. Silicon (Si) is a beneficial plant element that has been shown to mitigate the effects of potentially toxic elements (PTEs) on crops. Biochar is a soil amendment that sequesters soil carbon, and that can immobilize PTEs and enhance crop growth in soils. No previous studies have examined the potentially synergistic effect of Si and biochar on soil Ni chemical fractions and immobilization. Therefore, the aim of this study was to examine the interaction effects of Si levels and biochars, to alleviate soil Ni bioavailability and its corresponding uptake in corn (*Zea Mays*) in a calcareous soil. A 90-day factorial greenhouse study with corn was conducted. Si application levels were applied at 0 (S₀), 250 (S₁) and 500 (S₂) mg Si kg⁻¹ soil and biochar treatments (3% wt.) including rice husk (RH) and sheep manure (SM) biochars produced at 300°C and 500°C (SM300, SM500, RH300 and RH500). At harvest, corn shoot Ni-concentrations, soil chemical Ni fractions and DPTA-release kinetics were determined. Simultaneous utilization of Si and SM biochars led to a synergistic reduction (15-36%) of soluble and exchangeable soil Ni fractions compared to application of Si (5-9%) and SM (5-7%) biochars separately. The application of the Si and biochars also decreased DPTA-extractable Ni and corn Ni shoot concentration (by up to 57%), with the combined application of SM500+S₂ being the most effective. These effects were attributed to the transformation of Ni from more bioavailable fractions to more stable iron oxide bound fractions, related to soil pH increase. The SM500 was likely the most effective biochar due to its higher alkalinity and lower acidic functional group content which enhanced Ni sorption reactions with Si. The study demonstrates the synergistic potential of Si and sheep manure biochar at immobilizing Ni in contaminated calcareous soils.

1 Introduction

One of the most important ways for potentially toxic elements (PTEs) to enter the human food chain is through the consumption of plants grown in soils contaminated with PTEs. Potentially toxic elements pollute soil environments as a result of mining, metal smelting, using sewage sludge and domestic and industrial effluents in agriculture especially in developing countries (Liu et al., 2018). Potentially toxic elements in soils cannot undergo biodegradation by living organisms, so they possess great stability and longevity in the soil (Poznanović Spahić et al., 2019). Unlike other PTEs found in soils, such as mercury (Hg), cadmium (Cd) and lead (Pb),

43 nickel (Ni) is essential for plant growth at very low concentrations. Nevertheless, at elevated
44 contents ($>35 \text{ mg Ni kg}^{-1}$ soil), it causes many physiological and morphological malfunctions in
45 plants and severely stunts their growth (Shahzad et al., 2018; Antoniadis et al., 2017). In
46 agricultural soils of Iran in the vicinity of the industrial areas, the weighted average concentration
47 of Ni is 349.8 mg kg^{-1} soil. In these soils, the pollution index (the ratio of the element concentration
48 to the standard concentration) calculated for the Ni is greater than 5, which indicates a severe
49 degree of pollution from the point of view of environmental protection (Shahbazi et al., 2022).
50 Shahbazi et al. (2020) collected 711 agricultural soil samples from different climates of Iran and
51 reported that the Ni content in the soils was between 2.79 mg kg^{-1} and 770 mg kg^{-1} with an average
52 of 68 mg kg^{-1} soil. The results showed that the concentration of Ni in 11.3% of these soils was
53 higher than the threshold value. Removing PTEs from contaminated sites via traditional methods
54 such as pump and treat technologies, soil washing and excavation is very expensive and time-
55 consuming, therefore, for plant cultivation in these areas, low-cost and effective methods should
56 be sought to stabilize PTEs in soils and prevent them from being transferred to the plant (Gao et
57 al., 2023).

58 Silicon (Si) is a valuable nutrient for plant growth, and it is only considered essential for
59 some plant species such as rice. Applying Si to the soil can enhance plant resistance against
60 biological and non-biological tensions, including physiological stress caused by PTEs in soil (Bhat
61 et al., 2019; Yan et al., 2018). The use of Si to promote plant growth and mitigate PTEs toxicity is
62 becoming increasingly popular in agriculture (Li, 2019; Adrees et al., 2015). The application of Si
63 in soils contaminated with PTEs may reduce PTEs bioavailability by increasing soil pH, increasing
64 the secretion of organic ligands by the roots and forming insoluble compounds with PTEs, and
65 ultimately enhancing plant growth (Bhat et al., 2019; Xiao et al., 2021). The soil pH increase
66 associated with Si application is attributed to the hydrolysis reaction of the silicate anion in soil
67 solution which generates hydroxyl ions (Ma et al. 2021).

68 Biochar is an organic soil amendment that sequesters soil carbon (C) that has received
69 much attention in recent years to stabilize PTEs in polluted sites (El-Naggar et al., 2018). Biochar
70 is a carbon-rich, porous organic material which is prepared in a limited or no oxygen conditions
71 by pyrolysis of organic wastes, including crop and animal residues, urban waste, wood byproduct
72 (Vickers, 2017; Ankita Rao et al., 2023). The organic surface functional groups of biochar such as
73 carboxylic and phenolic groups provide cation exchange capacity in soils (Tomczyk et al., 2020).
74 Addition of biochar to the soil not only improves the soil chemical and physical properties, but
75 also reduces the bioavailability of PTEs in contaminated soils through some physicochemical
76 processes such as sedimentation, complexation, and electrostatic adsorption (Bandara et al., 2020;
77 Deng et al., 2019; Derakhshan Nejad et al., 2018). The complexation of Ni with oxygen-containing
78 functional groups on biochar surfaces including carboxyl, ether, carbonyl, and hydroxyl, has been
79 identified as a key mechanism for Ni immobilization in soil (Alam et al., 2018; El-Naggar et al.,
80 2018). Electrostatic attraction of Ni by negatively charged functional groups on the surfaces of
81 biochar is another potential mechanism for soil Ni stabilization (Ahmad et al., 2014). Increasing
82 soil pH following the application of biochar also promotes Ni adsorption reactions (Uchimiya et
83 al., 2010). However, the efficiency of biochar prepared from different feedstocks and under
84 different production conditions in stabilizing PTEs in soils can vary significantly (Dey et al., 2023).

85 Potentially toxic elements in soil can exist in different chemical fractions such as water
86 soluble and exchangeable (WsEx), bound to carbonates (CAR), organic materials (OM), iron and
87 manganese oxides (FeMnOx) and residual (Res) (found in minerals) (Singh et al., 1988). The

88 bioavailability of these forms differs, the WsEx fraction has the highest bioavailability and the Res
89 form is considered unusable by plants. The other chemical fractions of PTEs in soils could be
90 potentially accessible for plant roots depending on soil characteristics such as soil texture, soil pH
91 and soil organic matter content (Kamali et al., 2011; Bharti et al., 2018). The diethylene triamine
92 penta-acetic acid (DTPA) extraction is commonly employed for assessing Ni availability in
93 calcareous soils (Lindsay and Norvell, 1978). However, it is important to acknowledge that this
94 methodology solely assesses Ni availability for plants, while the quantity of released Ni may vary
95 across distinct stages of plant development. Consequently, the examination of alterations in
96 extractable Ni levels over time using the DTPA solution can prove valuable in estimating soil Ni
97 bioavailability. The PTE desorption capacities of soils are anticipated to be contingent upon factors
98 such as soil pH, cation exchange capacity, the specific nature of metal ions, and the source of the
99 metals (Kandpal et al., 2005). Furthermore, the release kinetic parameters can provide insight into
100 the mechanisms of PTEs bonding in soils and their potential risk for leaching into groundwater or
101 surface water (El-Naggar et al., 2021). Therefore, sequential extraction methods and release
102 kinetics models have been employed to assess the efficacy of amendment materials in stabilizing
103 PTEs in contaminated soils. Xiao et al. (2021) found that addition of mineral Si fertilizer to a
104 contaminated paddy soil caused a significant decrease in the Cd and Pb fractions bound to
105 carbonates and iron-manganese oxides while the forms of residual and bound to organic matter
106 increased. In another study, application of cotton residue biochar (1.5 wt. %) to a calcareous soil
107 with a light texture containing different levels of Cd contamination was more efficacious than corn
108 and wheat straw biochars in decreasing the WsEx-Cd and Car-Cd forms and enhancing the Res-
109 Cd form. In addition, application of cotton residue biochar decreased EDTA-extractable Cd by
110 45–52% compared to the control (Boostani et al., 2023a).

111 As both biochars and Si are economical and effective soil amendments to reduce plant PTE
112 uptake and stress in contaminated soils, their potential synergistic effect on the immobilization of
113 PTEs in soils should be further investigated. Currently, no previous studies have examined the
114 combined application effects of Si and biochars on the chemical fractions and release kinetics of
115 Ni in calcareous soils. The primary objective of the present study was to elucidate the interaction
116 of biochars and Si levels, to alleviate soil Ni bioavailability and its corresponding accumulation in
117 corn (*Zea Mays* L. 604) plant. Additionally, the study sought to elucidate the underlying soil
118 chemical mechanisms that are likely to be responsible for such effects.

119 **2 Materials and methods**

120 **2.1 Soil sampling, characterization and Ni treatment**

121 A composite soil sample from the surface layer (0-30 cm) was collected with an auger at
122 the research farm of the College of Agriculture and Natural Resources in Darab, southern Iran (28
123 ° 45' 0.99" N 54° 26' 52.14" E, Elevation 1105 m). The soil sample was air-dried, sieved
124 through a 2 mm mesh, and then physicochemical properties were determined. Soil sand, silt and
125 clay content were determined by sieving and the hydrometer method (Gee and Bauder, 1986). Soil
126 pH and EC were determined using a saturated paste (Rhoades, 1996), while organic matter was
127 determined using Walkley-Black procedure (Nelson and Sommers, 1996). Calcium carbonate
128 equivalent (CCE) was determined by acid neutralization (Loeppert and Suarez, 1996), while cation
129 exchange capacity was determined using 1M ammonium acetate (Merck, 99%) method (Sumner
130 and Miller, 1996). Available Ni was determined using DTPA (Merck, 99%) extraction (Lindsay
131 and Norvell, 1978). Plastic containers were filled with two kilograms of soil and then 500 mL
132 NiCl₂ (Merck, 99%) solution was mixed into to them to achieve a Ni concentration of 300 mg Ni

133 kg⁻¹ soil. The Ni-treated soil samples were then allowed to dry out at room temperature, and then
134 rewetted to field capacity using deionized water and allowed to dry out again. The rewetting and
135 room temperature drying cycle was repeated three times to allow the Ni to equilibrate with the soil
136 (Boostani et al., 2023c).

137 2.2 Production of biochar and its properties

138 The sheep manure and rice husk were respectively procured from an active animal
139 husbandry and rice mill factory situated in the Darab region, Fars province, Iran. Subsequently,
140 the raw materials underwent a 1-week period of air-drying, followed by electrical milling and
141 sieving through a 2 mm mesh. A slow pyrolysis procedure (2 h at 300 °C and 500 °C) in an oxygen-
142 limited environment was carried out to generate biochars from feedstocks (Anand et al., 2023).
143 The generated biochars were then cooled at ambient temperature and sieved with a 0.5 mm mesh
144 to ensure consistent particle size. The chemical characteristics of the biochars were assessed using
145 the following standard methods. Biochar pH and EC was determined in a 1:10 deionized water
146 suspension (Sun et al., 2014), while CEC was determined using the method of Abdelhafez et al.
147 (2014). Biochar total C, N and H contents was determined by elemental analyzer (ThermoFinnigan
148 Flash EA 1112 Series, ThermoFinnigan, USA). Biochar moisture and ash content were determined
149 by heating in an oven, while the O+S content was calculated by subtraction of C, N, H, ash and
150 moisture content from total biochar mass (Keiluweit et al., 2010). Biochar total Ni content was
151 determined by combustion and dissolution of the ash in 2M HCl (Merck, 37%) (Boostani et al.,
152 2018a). The Ni content in the acid solution was determined using atomic absorption spectroscopy
153 (AAS) (PG 990, PG Instruments Ltd., UK). The biochar surface functional groups were assessed
154 using Fourier Transform Infrared (FTIR) spectroscopy using a Shimadzu DR-8001 instrument and
155 KBr pellet transmission method. Biochar morphology was assessed using scanning electron
156 microscopy (SEM) (TESCAN-Vega3, Czech Republic).

157 2.3 Greenhouse experiment

158 A completely randomized factorial experiment was conducted in a greenhouse
159 environment with three replications. The first factor consisted of the biochar treatments including
160 rice husk (RH) and sheep manure (SM) generated at 300 °C and 500 °C (Control (C) (with no
161 biochar), SM300, SM500, RH300 and RH500), each at the rate of 3% wt. The second factor
162 included Si application levels (0 (S₀), 250 (S₁) and 500 (S₂) mg Si kg⁻¹ soil) supplied as Na₂SiO₃
163 (Sigma Aldrich, 98%) solution. Based on the experimental design, Si levels were added to the 2
164 kg of Ni-treated soil samples and after drying the soil and mixing it, the prepared biochars were
165 added to the required amount. Immediately after that, the treated soil samples were transferred to
166 plastic pots (45 pieces each containing 2 kg soil) and to facilitate the required reactions, the
167 moisture content of the samples was kept at field capacity level for a duration of two weeks.
168 Thereafter, 6 corn seeds (*Zea mays* L. 604) were planted in each pot, and at the 4-leaf stage, 2
169 plants were kept in each pot until the end of cultivation. During the growth of the plant, distilled
170 water was used to maintain the soil moisture content in the pots at field capacity. After 90 days,
171 the plants were harvested at the soil interface, rinsed with distilled water to remove contamination,
172 immediately air-dried and kept for Ni determination of plant shoots. After separating the roots
173 and air drying, the soil of the pots was sifted via a 2 mm mesh, and subsequently utilized for
174 performing Ni release kinetics experiment and determining the Ni chemical fractions.

175 2.4 Sequential extraction procedure

176 The present study employed a successive extraction technique (Singh et al., 1988) to
 177 fractionate soil nickel (Ni) in the following chemical forms, namely water-soluble and
 178 exchangeable (WsEx), carbonate-bound (Car), organic matter-bound (OM), manganese oxide-
 179 bound (MnOx), amorphous iron oxide-bound (AFeOx), crystalline iron oxide-bound (CFeOx), and
 180 residual (Res). The methodological specifics are provided in Table 1.

Table 1
 Successive extraction technique of Singh et al. (1988)

Chemical speciation containing Ni	acronym	Duration of agitation (h)	Extractants	Relative density (g.cm ⁻³)
Exchangeable and soluble	WsEx	2	1 M magnesium nitrate (Merck, 98%)	1.10
Carbonate	Car	5	1 M sodium acetate (Merck, 99%) (pH=5)	1.04
Organic	OM	0.5	0.7 M sodium hypochloride (pH=8.5)	1.00
Mn oxide	MnOx	0.5	0.1 M hydroxyl amine hydrochloride (Merck, 98%) (pH=2 by nitric acid (Merck, 65%))	1.00
Amorphous Fe oxides	AFeOx	0.5	0.25 M hydroxyl amine hydrochloride (Merck, 98%) + 0.25 M chloridric acid (Merck, 37%)	1.01
Crystalline Fe oxides	CFeOx	0.5	0.2 M ammonium oxalate (Merck, 99%) + 0.2 M oxalic acid (Merck, 99%) + 0.1 M ascorbic acid (Merck, 99.7%)	1.02

181

182 2.5 Release kinetics experiment

183 A fifty milliliters centrifuge tube was filled with 10 g of soil. After that, 20 ml of DTPA
 184 solution (0.005 M DTPA (Merck, 99%) + 0.1 M tri-ethanol amine (Merck, 99%) + 0.01 M calcium
 185 chloride (Merck, 97%)) (pH: 7.3) (Lindsay and Norvell, 1978) was added to the soil. The soil-
 186 DTPA mixtures were stirred for specific periods of time, i.e. 5, 15, 30, 60, 120, 360, 720 and 1440
 187 minutes at a constant temperature (25 ±2 °C). After each stirring time, the soil suspension was
 188 centrifuged (2683 × g) to separate the soil particles from the liquid phase. Atomic absorption
 189 spectroscopy (AAS) (PG 990, PG Instruments Ltd., UK) was used to analyze the Ni concentration
 190 in the liquid phase. The Ni concentration in the liquid phase versus time was plotted to obtain a Ni
 191 release kinetic curve. A total of seven kinetic models namely order models (zero, first, second and
 192 third), parabolic diffusion, power function and simple Elovich were assessed to fit the Ni release
 193 data. The best models for describing the data were selected according to the maximum value of
 194 the coefficient of determination (R²) and the minimum amount of the standard error of estimate
 195 (SEE)(Nasrabadi et al., 2022).

196 2.6 Data analysis

197 The ANOVA test was utilized to assess treatments effects in the individual and combined
 198 biochar and silicon treatments. Additionally, a comparison of means was conducted using the
 199 MSTATC computer program, applying Duncan's test with a significance level of 5%. Figures were
 200 generated using Excel 2013 software. Pearson correlation coefficients among parameters in the
 201 dataset were determined using SPSS 12.0.

202 3 Results and Discussion

203 3.1 Soil characteristics

204 The soil used in the study prior to experimental treatment, exhibited a sandy loam texture
205 and possessed alkaline properties with significant calcium carbonate content, while not being
206 classified as saline (Table 2). The quantity of soil organic matter was extremely low, a distinct
207 characteristic of soils from arid and semi-arid regions (Okolo et al., 2023) (Table 2). The relatively
208 low levels of clay and organic matter present in the soil contributed to a correspondingly low soil
209 cation exchange capacity (CEC) (Table 2). The soils in Iran mainly originate from calcareous
210 alluvium under xeric, ustic or aridic and mesic, thermic or hyperthermic moisture and temperature
211 regimes, respectively. These soils have varied properties such as calcium carbonate equivalent (1-
212 81%), clay content (1-75%), EC (0.4-49.0 dS m⁻¹), organic matter (0.1-21.5%) and gypsum content
213 (0-91%) (Ghiri et al., 2011). Furthermore, it should be noted that the concentration of available
214 soil Ni extractable by DTPA was very low (Table 2).

Table 2

Certain physicochemical attributes of the soil prior to cultivation.

Sand (%)	58.0
Silt (%)	30.0
Clay (%)	12.0
Soil textural class	Sandy loam
pH _(s)	7.59
EC (dS m ⁻¹)	2.60
CCE (%)	55.0
OM (%)	0.50
CEC (cmol ₍₊₎ kg ⁻¹)	11.7
Total Ni (mg kg ⁻¹)	28
Ni-DTPA (mg kg ⁻¹)	0.39

Notes: EC, electrical conductivity; OM, organic matter; CCE, calcium carbonate equivalent; CEC, cation exchange capacity.

215

216 3.2 Chemical characteristics of the biochars

217 As the pyrolysis temperature rose from 300 °C to 500 °C, the SM biochars demonstrated
218 elevated pH and EC values, with the highest levels observed at the highest temperature (Table 3).
219 The elevated levels of alkali salts, which are reflected in the high ash content (Table 3), are the
220 contributing factor behind this observation in the SM biochars in comparison to the RH biochars.
221 Plant-based biochars commonly exhibit reduced levels of dissolved solids in comparison to
222 animal-based biochars (Sun et al., 2014). The SM300 biochar possessed the highest CEC value of
223 19.70 cmol₍₊₎ kg⁻¹. The observed phenomenon may be attributed to the diminution of surface
224 functional groups, namely carboxyl and phenol, at elevated pyrolysis temperatures. These groups
225 are predominantly responsible for facilitating the cation exchange capacity (CEC) of biochars
226 (Tomczyk et al., 2020). As the pyrolysis temperature increased, there was an observed increase in
227 the C content of the biochars, and a corresponding decrease in the content of hydrogen, oxygen,
228 and nitrogen (Table 3). The observed increase in the concentration of C as pyrolysis temperature
229 rises is consistent with a concomitant rise in the degree of carbonization. The observed reduction
230 in the levels of H and O might be attributed to the occurrence of dehydration reactions,
231 decomposition of oxygenated bonds, and the liberation of low molecular weight byproducts rich

232 in H and O, as recently noted by Zhao et al. (2017). Nitrogen compound volatilization explains the
 233 diminished N content of the biochars at elevated pyrolysis temperatures. The ratios of H:C and
 234 O:C are significant indicators of the aromaticity and polarity of biochars; the lower the ratios the
 235 more condensed aromatic C the biochar contains (Chatterjee et al., 2020). The results shown in
 236 Table 3 indicated that the H:C and O:C mole ratios showed a gradual decrease as the pyrolysis
 237 temperature was increased, which can be interpreted as a sign of improved carbonization of the
 238 biochars (Zhao et al., 2017). The Ni content in the biochars derived from rice husk was below
 239 detection, whereas a limited quantity of Ni was detected in the biochars produced from sheep
 240 manure (Table 3).

Table 3
 Some physical and chemical properties of the biochars.

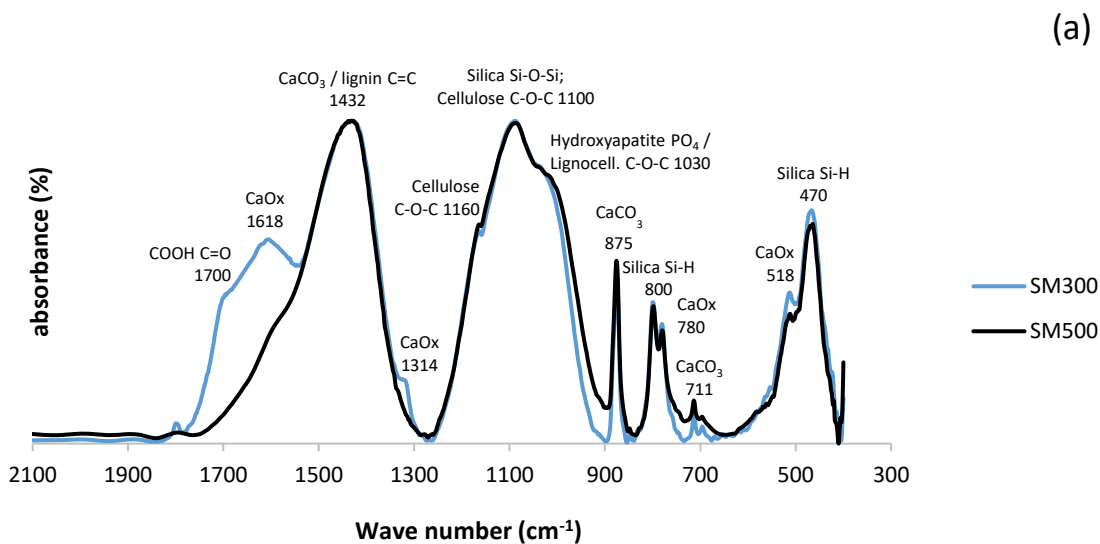
	SM300	SM500	RH300	RH500
pH (1:20)	9.96	11.0	9.0	10.3
EC (1:20) (dS m ⁻¹)	3.94	4.28	0.84	1.17
CEC (cmol _c kg ⁻¹)	19.70	18.94	18.94	15.33
C (%)	25.4	31.8	45.0	50.0
H (%)	1.85	0.8	2.28	1.06
N (%)	2.10	1.57	1.30	1.10
Ni (mg kg ⁻¹)	3.0	15.4	Nd	Nd
Moisture content (%)	1.91	1.82	2.65	2.37
Ash content (%)	53.8	60.0	34.2	44.8
H:C mole ratio	0.87	0.30	0.60	0.25
O+S:C mole ratio	0.44	0.09	0.24	0.01

Notes: SM300, sheep manure biochar generated at 300 °C; SM500, sheep manure biochar generated at 500 °C; RH300, rice husk biochar produced at 300 °C; RH500, rice husk biochar produced at 500 °C; CEC, cation exchange capacity; EC, electrical conductivity; Nd, non-detectable.

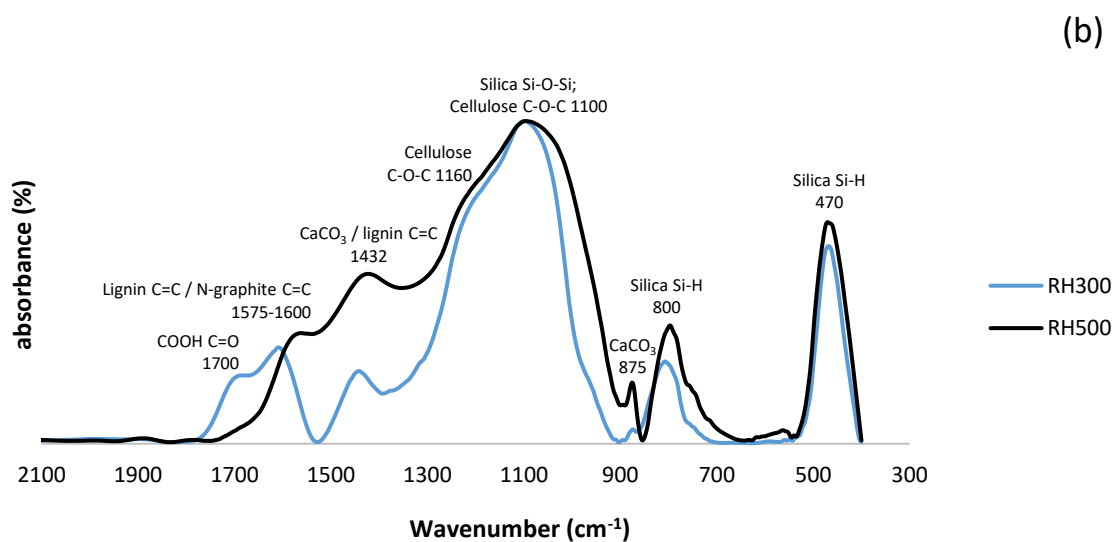
241

242 3.3 FTIR and SEM of the biochars

243 The FTIR spectra of the SM and RH biochars are shown in Figure 1. The SM and RH
 244 biochars produced at 300 °C contained a higher content of carboxyl groups (1700 cm⁻¹) (Keiluweit
 245 et al., 2010) than the biochars produced at 500 °C, which is in agreement with the O:C values of
 246 the biochars (Table 3). All of the biochars contained absorption bands associated with lignin (1430
 247 cm⁻¹) and cellulose (1030 -1160 cm⁻¹) (Keiluweit et al., 2010). The SM biochar contained more
 248 calcite than the RH biochar as indicated by the greater intensity of calcite characteristic peaks at
 249 1432, 875, and 711cm⁻¹ (Myszka et al., 2019) in the SM biochars (Fig. 1a). There was also
 250 evidence of the presence of Ca oxalate in the SM biochars, indicated by the characteristic peaks at
 251 1618, 780 and 518 cm⁻¹ (Maruyama et al., 2023). All the biochars contained silica as indicated by
 252 the intense silica absorption peaks at 1100, 800 and 470 cm⁻¹ (Zemnukhova et al., 2015).



253

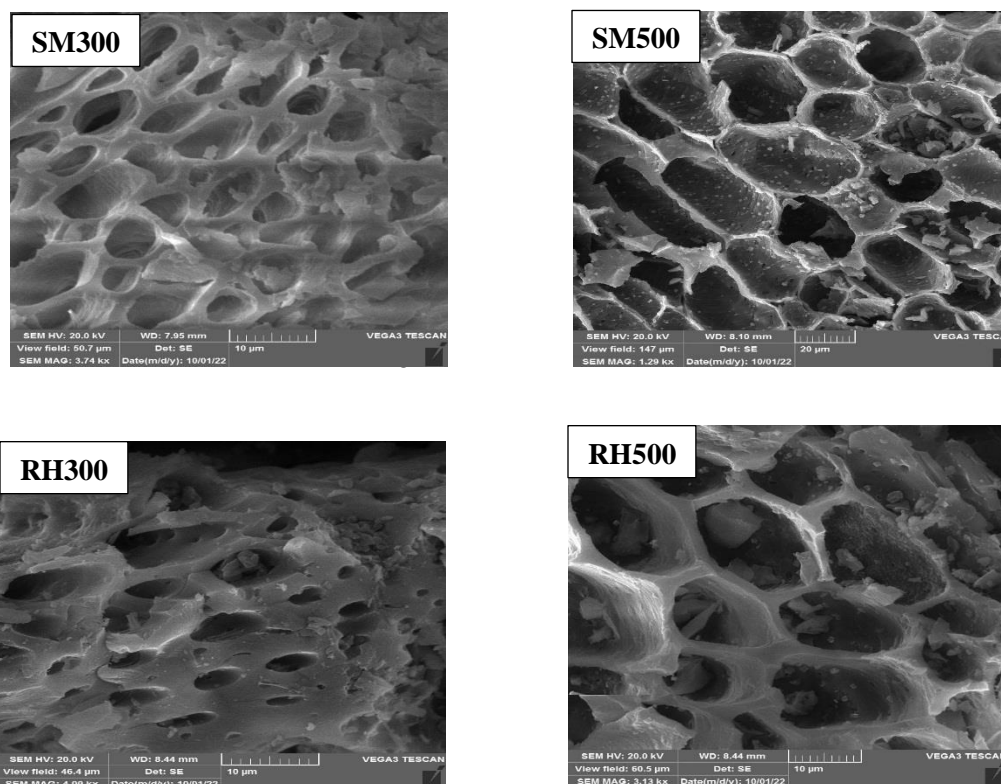


254

255 **Fig. 1.** FTIR of the biochars in the wave number range of 400–2000 cm^{-1} . Notes: SM300, sheep manure
 256 biochar produced at 300 °C; SM500, sheep manure biochar produced at 500 °C; RH300, rice husk biochar produced
 257 at 300 °C; RH500, rice husk biochar produced at 500 °C.

258

259 The SEM images of the SM and RH biochars are shown in Figure 2. The morphology of
 260 the biochars became more rigid and porous at higher temperatures, as evidenced by the cell wall
 261 shrinkage attributed to devolatilization of organic tissues (Claoston et al., 2014).



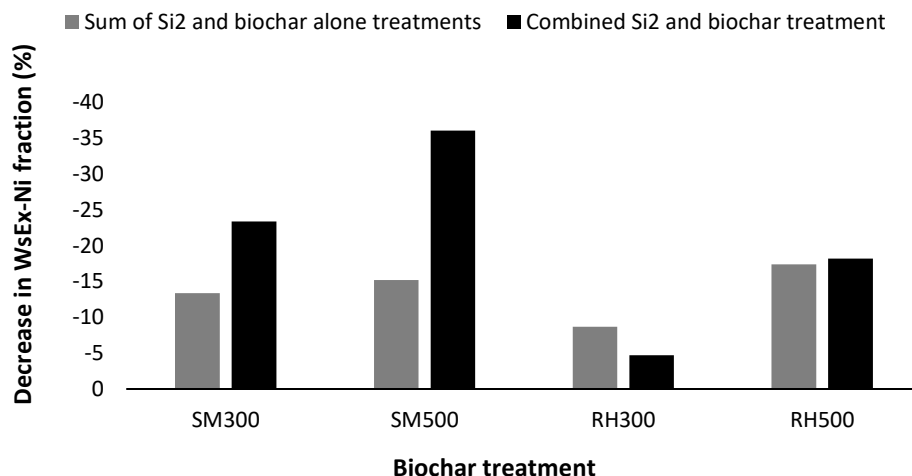
263

264 **Fig. 2.** SEM of the biochars. Notes: SM300, sheep manure biochar produced at 300 °C; SM500, sheep manure
 265 biochar produced at 500 °C; RH300, rice husk biochar produced at 300 °C; RH500, rice husk biochar produced at 500
 266 °C.
 267

268 3.4 Soil Ni chemical fractions after the addition of silicon and biochars

269 The main effects of treatments (biochars and Si levels) and their interactions had a
 270 statistically significant effect ($P < 0.01$) on all the soil Ni chemical fractions, except for the Ni-Car
 271 fraction, where only the main effects were significant. The soil Ni concentration in the WsEx
 272 fraction was significantly reduced by the application of Si rates from S_0 to S_2 by 14.8% (Table 4).
 273 Among the biochar treatments, the greatest decrease in WsEx-Ni fraction compared to the control
 274 was due to SM500 by 17%, while the RH300 treatment had no significant effect (Table 4). The
 275 interaction effect of treatments indicated that the lowest WsEx-Ni concentration was due to the
 276 combined treatment of SM500+ S_2 ($4.04 \text{ mg Ni kg}^{-1} \text{ soil}$) (Table 4). The combined treatment of S_2
 277 and SM biochars had strong synergistic effect on reducing WsEx-Ni fraction (23-36% reduction)
 278 compared to the sum of the treatments alone (13-15% reduction) (Fig. 3). Whereas this synergistic
 279 effect of the combined treatments was not evident for the RH biochars (Fig. 3). There was a
 280 negative correlation between soil WsEx fraction and soil pH ($r = -0.66, p < 0.01$) indicating
 281 that the reduction in WsEx fraction was strongly linked to the increase in soil pH due to the
 282 amendments. Previous studies have also shown that application of biochars and silicates result in
 283 increases in soil pH, thus reducing the bioavailability of PTEs and their conveyance to plant roots
 284 (Shen et al., 2020; Ma et al., 2021). Among the applied biochars, the maximum pH and ash content
 285 (Table 3) and calcite (lime) content (Fig. 1) were attributed to the SM500 biochar. Therefore, the
 286 combined SM500+ S_2 was most effective at reducing WsEx-Ni fraction, likely due to the higher

287 alkalinity and ash content of SM500 promoting Ni precipitation and adsorption (Sachdeva et al.,
288 2023).



289
290 **Fig. 3.** Comparison of the effect of sum of the Si₂ and biochar alone treatment versus the combined
291 Si₂ and biochar treatments on the % reduction of the WsEx-Ni fraction. Notes: SM300, sheep manure
292 biochar produced at 300 °C; SM500, sheep manure biochar produced at 500 °C; RH300, rice husk biochar produced
293 at 300 °C; RH500, rice husk biochar produced at 500 °C.

294 The reduced effectiveness of biochars produced at 300 °C, as compared to those produced
295 at 500 °C, in decreasing soil Ni-WsEx content could probably be attributed to the lower rates of
296 microbial oxidation and mineralization of RH500 and SM500, which is indicated by their higher
297 environmental stability (as reflected by lower H/C mole ratio values) (Table 3). Consequently,
298 biochar produced at 500 °C may not provide sufficient acidic carboxyl functional groups to the
299 soil to stimulate SOM decomposition, leading to a greater increase in soil pH (Sun et al., 2023).
300 According to Zhu et al. (2015), the addition of wine lees-based biochar (a material from a wine
301 processing factory) to a heavy metal-contaminated soil (at rates of 0.5% and 1% w/w) resulted in
302 an increase in soil pH and a decrease in the soil Ni content in the WsEx fraction. Furthermore, the
303 increase in soil pH due to the increase in Si levels may lead to the precipitation of Ni in the forms
304 of Ni silicate and hydroxide. Due to the high solubility of Na metasilicate, the hydrolysis of silicate
305 anion in the soil solution is intensified, leading to a high concentration of OH⁻ and a subsequent
306 increase in soil pH (Ma et al., 2021).

307
308
309
310
311
312
313

Table 4

Effects of biochars and silicon levels on the soil Ni chemical fractions (mg kg⁻¹) and Ni mobility factor (%) after corn cultivation.

	C	SM300	SM500	RH300	RH500	Mean
WsEx						
S ₀	6.32 a	6.02 a-c	5.91 bc	6.31 a	5.77 c	6.07 A
S ₁	6.03 a-c	5.37 d	5.09 de	6.25 ab	5.28 d	5.60 B
S ₂	5.77 c	4.84 e	4.04 f	6.02 a-c	5.17 de	5.17 C
Mean	6.04 A	5.41 B	5.01 C	6.20 A	5.41 B	
OM						
S ₀	9.72 a	10.15 a	8.04 d-f	10.08 a	9.02 b	9.40 A
S ₁	9.60 a	9.75 a	7.16 g	8.62 b-d	8.70 bc	8.76 B
S ₂	8.11 c-f	7.94 ef	7.12 g	8.30 c-e	7.63 fg	7.82 C
Mean	9.14 A	9.28 A	7.44 C	8.99 A	8.44 B	
MnOx						
S ₀	11.58 a	3.77 kl	5.99 f	4.69gh	9.71 c	7.15 A
S ₁	10.33 b	3.50 l	5.00 g	4.57 hi	8.93 d	6.48 B
S ₂	10.28 b	2.98 m	4.28 ij	3.96 jk	7.94 e	5.89 C
Mean	10.73 A	3.42 E	5.09 C	4.41 D	8.86 B	
AFeOx						
S ₀	11.15 ef	10.38 g	11.83 d	10.96 fg	11.75 de	11.21 C
S ₁	12.20 b-d	10.73 fg	12.03 cd	12.20 b-d	12.66 bc	11.96 B
S ₂	12.84 b	12.18 b-d	12.16 b-d	12.31 b-d	14.25 a	12.74 A
Mean	12.06 B	11.09 C	12.00 B	11.82 B	12.88 A	
CFeOx						
S ₀	77.32 f	77.98 f	83.97 cd	84.67 cd	79.60 ef	80.67 C
S ₁	77.89 f	82.20 de	86.34 bc	85.12 b-d	83.62 cd	83.03 B
S ₂	79.92 ef	85.50 bc	87.88 ab	85.69 bc	90.40 a	85.88 A
Mean	78.37 C	81.89 B	86.00 A	85.16 A	84.54 A	
Res						
S ₀	199.7 c-e	207.5 a	199.8 c-e	196.5 f	197.8 d-f	200.3 A
S ₁	199.9 c-e	204.5 b	200 cd	197.3 ef	195.5 f	199.5 A
S ₂	200.3 cd	204.1 b	201 c	199.4 c-e	190.4 g	199 A
Mean	200 B	205.4 A	200.3 B	197.7 B	194.6 BC	

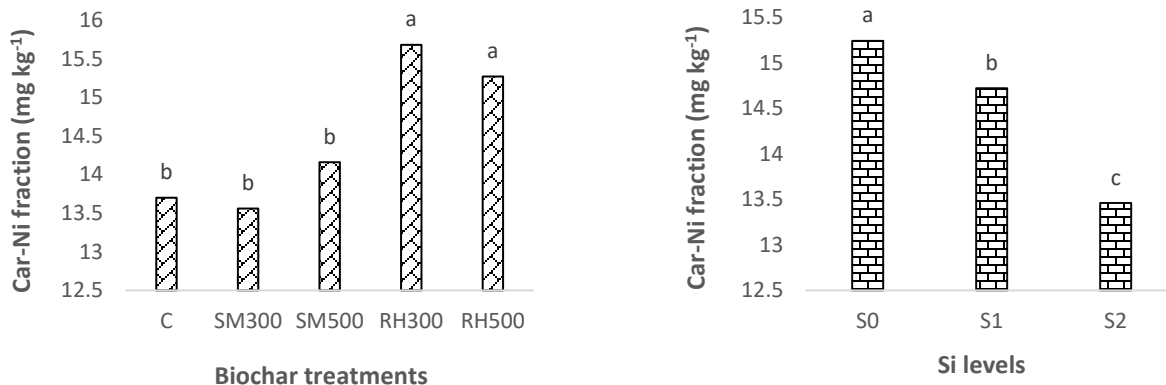
Notes: C, control; SM300, sheep manure biochar produced at 300 °C; SM500, sheep manure biochar produced at 500 °C; RH300, rice husk biochar produced at 300 °C; RH500, rice husk biochar produced at 500 °C; S₀, without Si addition; S₁, application of 250 mg Si kg⁻¹ soil; S₂, application of 500 mg Si kg⁻¹ soil. WsEx, water soluble and exchangeable fraction; OM, organic fraction; MnOx, bound to manganese oxides; AFeOx, bound to amorphous iron oxides; CFeOx, bound to crystalline iron oxides; Res, residual fraction; MF, mobility factor.

*Numbers followed by same letters in each column and rows, in each section, are not significantly (P<0.05) different

314 Application of Si rates from S₀ to S₂ significantly decreased the soil Ni content in the Car
315 fraction by 11.70% (from 15.24 mg Ni kg⁻¹ soil to 13.46 mg Ni kg⁻¹ soil) (Figure 4). The SM
316 biochars had no significant effect on the Car-Ni fraction whereas addition of RH biochars led to a
317 significant increase in this fraction (Figure 4). Ippolito et al. (2017) found that addition of two
318 biochars (pine [*Pinus contorta*] and tamarisk [*Tamarix* spp.]) to a mine contaminated soil caused
319 a significant increase in the soil Cd content bound to carbonates. They concluded that the reduction
320 in Cd bioavailability may have been due to the ability of biochar to raise soil pH levels and induce
321 the precipitation of CdCO₃. Similarly, Yuan et al. (2011) proposed that the decrease in PTEs
322 bioavailability in soil might have been caused by the creation of metal-carbonate species and
323 carbonate-surface functional group reactions, which could function as a mechanism for
324 sequestration. The decrease in the concentration of Ni in the carbonate form with an increase in

325 the Si levels could potentially be explained by the competition between silicate (SiO_4^{4-}) and
 326 carbonate ions for binding with Ni^{+2} ions in the soil solution (Sparks et al., 2022).

327



328

329 **Fig. 4.** Effects of (a) biochars and (b) silicon levels on the soil Ni concentration (mg kg^{-1}) in the
 330 carbonate-bound fraction after corn cultivation. Notes: C, control; SM300, sheep manure biochar produced
 331 at 300 °C; SM500, sheep manure biochar produced at 500 °C; RH300, rice husk biochar produced at 300 °C; RH500,
 332 rice husk biochar produced at 500 °C; S₀, without Si addition; S₁, application of 250 mg Si kg^{-1} soil; S₂, application of
 333 500 mg Si kg^{-1} soil. * Numbers followed by same letters in each section, are not significantly ($P < 0.05$) different.

334

335 The biochars produced at 300 °C had no significant effect on the OM-Ni fraction compared
 336 to control, while the biochars generated at 500 °C significantly decreased it (Table 4). The greatest
 337 OM-Ni reduction (18.6%) was due to SM500. Lu et al. (2017) explored how the application of
 338 bamboo and rice straw biochars with varying mesh sizes (0.25 and 1 mm) and at three different
 339 rates (0, 1, and 5% w/w) affected the distribution of Cd in a contaminated sandy loam soil, using
 340 the BCR (Bureau Communautaire de Référence) sequential extraction method. In contrast to the
 341 present study, they reported that the biochars increased the concentration of the Cd-OM fraction
 342 as affected, and that this was closely related to the increase in Cd immobilization. In another study,
 343 the application of sheep manure biochar produced at 500 °C at the rate of 3% (w/w) to a Cd-
 344 contaminated calcareous soil resulted in a significant increase in the OM-Cd fraction, whereas the
 345 addition of other biochar treatments (wheat straw, corn straw, rice husk, licorice root pulp) caused
 346 a significant decrease in the concentration of Cd in the OM form when compared to the control
 347 soil (Boostani et al., 2018b). In the study conducted by Boostani et al. (2018), the reduction in
 348 OM-Cd fraction as affected by application of rice husk biochar is in line with our results, however;
 349 the increase in soil OM-Cd content with addition of sheep manure biochar is in conflict with the
 350 result of the present study. According to the above-mentioned points, it seems that, in addition to
 351 the characteristics of biochar and the level of its application (Lu et al., 2017), soil characteristics
 352 (calcium carbonate percentage, soil texture, etc.) and the type of heavy metal can also have a
 353 substantial role in the binding of PTEs to soil organic matter. By increasing the Si rates from S₀ to
 354 S₂, the OM-Ni fraction was reduced by 16.8% (Table 4). It has been shown that the application of
 355 Si to cultivated soils resulted in a reduction of soil organic matter content. This implies that Si

356 facilitates the decomposition and accessibility of organic matter to plants (Ma et al., 2021). The
357 interaction effects of biochars and Si levels showed that the lowest OM-Ni concentration was due
358 to the combined treatment of SM500+S₂ (7.12 mg Ni kg⁻¹ soil), which was equal to a 26.7%
359 decrease compared to the combined treatment of C+S₀ (9.72 mg Ni kg⁻¹ soil) (Table 4).

360 All the biochar treatments caused a significant decrease in MnOx-Ni fraction compared to
361 control, with the greatest reduction was attributed to the SM300 by 52.6% (Table 4). The lower
362 temperature biochars were more effective than the higher temperature biochars in decreasing the
363 MnOx-Ni fraction (Table 4). In agreement with the present study, Boostani et al. (2023c) observed
364 that biochars produced from cow manure, municipal solid waste and licorice root pulp at lower
365 pyrolysis temperature (300 °C) decreased the soil Ni content in the MnOx fraction to a greater
366 extent than those prepared at higher temperature (600 °C). Hydrophobicity of biochar is decreased
367 with increasing the pyrolysis temperature (Kameyama et al., 2019). At the same soil water content,
368 the water content of soil pores treated with biochars produced at low pyrolysis temperature is
369 higher due to lower absorption of water by the biochars. Therefore, in soils with high soil pore
370 water content and low oxygen conditions, the concentration of MnOx is decreased due to chemical
371 reduction, while concomitantly, the exchangeable and water-soluble Mn concentration are
372 increased (Sparrow and Uren, 2014). Furthermore, increasing the Si concentration from S₀ to S₂
373 significantly decreased MnOx-Ni by 17.6% (Table 4). The interaction effect of treatments showed
374 that the highest and the lowest MnOx-Ni concentrations were found in the untreated control (11.58
375 mg Ni kg⁻¹ soil) and combined SM300+S₂ (2.98 mg Ni kg⁻¹ soil), respectively (Table 4). The
376 concentrations of soil Ni bound to AFeOx and CFeOx were significantly increased by application
377 of Si levels from S₀ to S₂ by 13.6% and 6.5%, respectively (Table 4). Belton et al. (2012)
378 demonstrated that exogenous silicon application resulted in the attachment of silicate to the surface
379 of iron oxide in the form of a polymer. Following the complexation of ferrosilicon, a significant
380 number of negatively charged functional groups, including silanol, were formed. These groups
381 provided numerous adsorption sites for PTEs, ultimately reducing their bioavailability (Belton et
382 al., 2012). In general, all the biochars caused a significant increase in CFeOx-Ni fraction, and there
383 were no significant differences among the SM500, RH300 and RH500 treatments (Table 4).
384 However, the only the RH500 treatment increased the AFeOx-Ni concentration of soil compared
385 to control (Table 4). Among all the biochars, only the SMB300 resulted in a significant increase
386 in the soil Ni concentration in the Res fraction compared to the control (Table 4). The application
387 of Si also did not significantly effect this form (Table 4).

388 Mailakeba and Bk (2021) studied the addition of kunai grass biochar (0.75%) to a soil with
389 different Ni contamination levels (0, 56, 100, and 180 mg Ni kg⁻¹ soil). They found that the
390 application of the grass biochar increased the Res-Ni fraction and reduced the WsEx and OM-Ni
391 fractions. In another study, Boostani et al. (2023c) demonstrated that the application of biochars
392 (cow manure, municipal compost and licorice root pulp each at 3%(w/w)) to a Ni-contaminated
393 soil increased the concentrations of OM-bound and residual Ni fractions, and decreased the
394 concentrations of WsEx, Car, and Fe/Mn oxide-bound Ni fractions. Whereas, Boostani et al.
395 (2023b) found that the application of manure and compost biochars (3% w/w) to Pb-contaminated
396 soil did not significantly affect the Res-Pb fraction but did decrease the WsEx fraction. Therefore,
397 it seems that the effect of biochars on the transformation of soil PTE chemical fractions depends
398 on the raw materials and production conditions of the biochar, the soil application rates, type of
399 PTEs, the degree of soil contamination with PTEs, the selection of sequential extraction procedure
400 and the soil properties (Mailakeba and Bk, 2021; Boostani et al., 2023a, b; Boostani et al., 2021).

401 In summary, the application of biochars in the present study resulted in the transformation
402 of Ni in the soil from more bioavailable and mobile fractions (WsEx, MnOx, OM) to more stable
403 forms (AFeOx and CFeOx). These changes were particularly evident in the WsEx fraction when
404 SM biochar was applied in conjunction with silicon, indicating that the simultaneous use of these
405 two substances was much more effective than applying them separately.

406 3.5 Shoot Ni concentration of *Zea mays L.* as affected by treatments

407 The main effects of biochars, Si rates and their interactions were statistically significant on the
408 shoot Ni concentration of the corn. Addition of Si levels from S₀ to S₂ resulted in 32% decrease in
409 shoot Ni concentration (Table 5). In addition, the shoot Ni concentration was significantly
410 decreased by application of all the biochar treatments compared to the control (with no biochar
411 addition) (Table 5). The interaction effects of treatments showed that the highest and lowest shoot
412 Ni concentration were due to the combined treatments of C+S₀ (10.4 mg Ni kg⁻¹ DM) and
413 SM500+S₂ (4.45 mg Ni kg⁻¹ DM), respectively (Table 5). The shoot Ni concentration had a
414 significant and positive correlation with the Ni-WsEx fraction ($r = +0.62$, $P < 0.01$) while there
415 were a significant and negative correlation between the soil pH ($r = -0.60$, $P < 0.01$) and Ni-
416 CFeOx fraction ($r = -0.50$, $P < 0.01$). This indicates that the application of Si and biochar can
417 reduce the shoot Ni concentration by increasing soil pH and, as a result, reducing the amount of
418 Ni in the fraction of WsEx and increasing the Ni content attached to crystalline iron oxides.
419 Boostani et al. (2019a) reported the reduction of shoot Ni concentration of spinach (*Spinacia*
420 *oleracea* L.) due to the application rice husk and licorice root pulp biochars (2.5% w/w) application
421 in a Ni-contaminated calcareous soil. Additionally, they reported that the biochars produced at 350
422 °C were more effective at reducing crop Ni uptake and promoting plant growth than the biochars
423 produced at 550 °C. The most significant factors that contribute to the reduction of PTE-uptake by
424 plants in contaminated soils that have been amended with biochars include surface adsorption of
425 heavy metals, increased soil pH, altered redox conditions of PTEs, improved physical and
426 biological properties of the soil, changes in the activity levels of antioxidant enzymes, and a
427 decrease in the transfer of PTEs to the plant shoots (Zeng et al., 2018; Rizwan et al., 2016). Several
428 studies have investigated the effect of Si application on shoot Ni concentration and other heavy
429 metals in various plant species. Khaliq et al. (2016) observed a notable increase Ni concentration
430 and accumulation within the leaf, stem, and roots of cotton after Ni application. Whereas, Si
431 application was observed to induce a significant reduction in Ni concentrations across these
432 respective plant components. In another study, Maryam et al. (2024) concluded that addition of Si
433 caused an increase in the growth indices of maze through reducing the Pb-shoot concentration.
434 One possible explanation for the reduction in shoot Ni concentration is that Si can compete with
435 Ni for uptake by plant roots. Silicon has a similar ionic radius to Ni, which means that it can occupy
436 the same binding sites on root cell membranes and reduce the uptake of Ni. Additionally, Si can
437 induce the expression of genes that are involved in Ni transport and homeostasis, which may
438 contribute to the reduced shoot Ni concentration (Hossain et al., 2012; Liang et al., 2005).

439

440

441

Table 5Shoot Ni concentration (mg Ni kg⁻¹ DM) as affected by biochars and silicon application levels.

	C	SM300	SM500	RH300	RH500	
S ₀	10.4 a	7.35 bc	9.85 a	7.55 bc	7.65 b	8.56 A
S ₁	7.65 b	6.90 bc	6.60 cd	7.05 bc	7.35 bc	7.11 B
S ₂	7.20 bc	5.05 ef	4.45 f	5.80 de	6.60 cd	5.82 C
Mean	8.41 A	6.43 C	6.96 BC	6.80 BC	7.20 B	

Notes: C, control; SM300, sheep manure biochar generated at 300 °C; SM500, sheep manure biochar generated at 500 °C; RH300, rice husk biochar produced at 300 °C; RH500, rice husk biochar produced at 500 °C; S₀, without Si application; S₁, addition of 250 mg Si kg⁻¹ soil; S₂, addition of 500 mg Si kg⁻¹ soil. Numbers followed by same letters in each section, are not significantly (P<0.05) different.

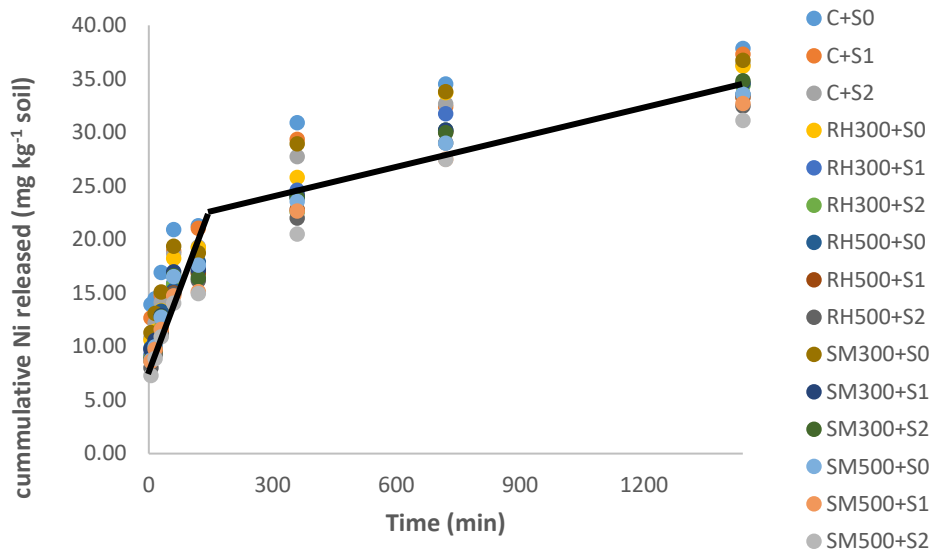
442

443 3.6 Soil Ni desorption as affected by Silicon levels and biochars

444 The cumulative soil Ni desorption (extracted by DTPA) as a function of time are shown in
 445 Fig. 5. The release of Ni from the soil initially proceeded at a much higher rate during the first
 446 hour, and then proceeded at a much slower rate during the next 24 hours, as illustrated by the trend-
 447 line in Fig. 5. This two-stage process of releasing heavy metals from soil has also been reported
 448 by other researchers (Sajadi Tabar and Jalali, 2013; Boostani et al., 2023a). It is likely that the
 449 first stage of release is related to forms of Ni that are less strongly attached to soil particles,
 450 including WsEx and Car, while the second stage of desorption is likely from fractions of Ni with
 451 less bioavailability, such as FeOx and Res (Saffari et al., 2015). In general, the amount of soil Ni
 452 desorption was reduced by addition of biochars and Si levels (Fig. 5). In addition, the effects of
 453 biochars produced at higher pyrolysis temperature (500 °C) on reducing the soil Ni release was
 454 more than those generated at lower pyrolysis temperature (300 °C). The highest amount of soil Ni
 455 release was due to the combined treatment of C+S₀ (37.84 mg Ni kg⁻¹ soil) while the lowest was
 456 observed in the combined application of SM500 and S₂ (31.13 mg Ni kg⁻¹ soil) treatment.

457

458



459

460 **Fig. 5.** Cumulative soil Ni desorption (extracted by DTPA) (mg kg^{-1}) as affected by different
 461 treatments. Notes: C, control; SM300, sheep manure biochar produced at 300°C ; SM500, sheep manure biochar
 462 produced at 500°C ; RH300, rice husk biochar produced at 300°C ; RH500, rice husk biochar produced at 500°C ; S₀,
 463 without Si addition; S₁, application of $250 \text{ mg Si kg}^{-1}$ soil; S₂, application of $500 \text{ mg Si kg}^{-1}$ soil.

464 3.7 Fitting of Ni release data to kinetics models

465 The soil Ni release data during 24 hours for all the biochar and Si treatments were evaluated
 466 by seven different kinetic models (Table 6). The effectiveness of the various kinetic models to
 467 describe the observed soil Ni desorption was analyzed by considering the coefficient of
 468 determination (R^2) and standard error of estimate (SEE), so that the highest value of the R^2 and the
 469 lowest value of the SEE were set as the criteria. As seen in Table 6, the order kinetic models did
 470 not adequately describe soil Ni release, and with the increase in the order of the kinetic model
 471 (from zero to third), the value of the R^2 decreased. This has also been found by other researchers
 472 for the release of heavy metals from soil (Boostani et al., 2019b; Ghasemi-Fasaee et al., 2006).
 473 Whereas, the non-order kinetic models, including power function, parabolic diffusion and simple
 474 Elovich, acceptably described the soil Ni release of the various treatments (Table 6). Among them,
 475 the power function model was the best according to the highest value of R^2 (0.98) and the lowest
 476 value of SEE (0.055). Boostani et al. (2018b) also reported that the power function was the best
 477 kinetic model to describe soil Cd desorption from a Cd-contaminated soil treated with biochars
 478 and zeolite.

479

480

481

482

483

484

Table 6

The range of coefficients of determination (R^2) and standard error of estimate (SEE) of applied kinetic models to all the soil treatments.

Kinetic models	R^2		SEE	
	Range	Mean	Range	Mean
Zero order	0.79-0.87	0.80	3.36-4.67	3.67
First order	0.69-0.75	0.75	0.22-0.29	0.25
Second order	0.53-0.61	0.52	0.011-0.026	0.0018
Third order	0.39-0.51	0.41	0.0013-0.0052	0.0030
Parabolic diffusion	0.94-0.98	0.96	1.26-2.44	1.85
Power function	0.97-0.99	0.98	0.054-0.057	0.055
Simple Elovich	0.92-0.97	0.95	2.04-2.78	2.50

485

486 3.8 Using the parameters of power function model to investigate the effect of treatments on soil
487 Ni desorption

488 As the power function model ($q = at^b$) described the soil Ni release data the best, its
489 parameters (a and b) were used to investigate the effect of biochar application and Si levels on the
490 release of Ni from the Ni-contaminated soil (Table 7). The main effects of biochars and Si levels
491 and their interactions on the 'a' and 'b' parameters were significant ($P < 0.01$). As Dang et al.
492 (1994) reported, in this kinetics model, a decrease in parameter 'a' and an increase in parameter 'b'
493 indicates a decrease in the rate of heavy metals desorption from the soil. The main effects of
494 treatments showed that addition of all the biochar treatments caused a significant decrease in the
495 'a' parameter compared to the control while the 'b' parameter was significantly increased (Table
496 7). The same trend was observed for all the Si treatment rates (Table 7). Therefore, it can be
497 concluded that the use of all the biochars and Si levels has caused a decrease in the rate of Ni
498 release from the Ni-contaminated soil. Generally, there was a greater decrease in Ni desorption in
499 biochar treatments prepared at the higher temperature (Table 7). The interaction effects indicated
500 that the most effective combined treatment in reducing the rate of Ni release from the soil was
501 SM500+S₂ which had the lowest value of parameter 'a' (4.52) and the highest value of parameter
502 'b' (0.264) among the treatments.

503 If it is differentiated from the power function equation ($q = at^b$) with respect to time (t)
504 ($dq/dt = ab t^{b-1}$), when $t = 1$ s = 0, the ratio of dq/dt becomes 'ab'. This parameter indicates the
505 amount of heavy metal desorption in the initial time (Dalal, 1985). The 'ab' parameter was affected
506 by the application of Si levels and biochars, so that this parameter was significantly decreased
507 compared to the control with addition of all the biochars (12.4%, 24.2%, 15.4% and 21.3% for the
508 SM300, SM500, RH300 and RH500, respectively) and Si rates (13% from S₀ to S₂), (Table 7).
509 This finding also confirmed the effect of applied treatments in reducing the amount of Ni release.
510 The greatest reduction was observed in the combined treatment of SM500+S₂ by 33.5% compared
511 to the control (Table 7).

512

513

514

515

Table 7

The coefficients of power function model as affected by biochars and silicon levels in a Ni-polluted calcareous soil after corn cultivation.

	C	SM300	SM500	RH300	RH500	
	a (mg Ni kg ⁻¹ h ⁻¹) ^b					
S ₀	9.15 a	7.39 c	5.56 gh	6.49 e	5.95 f	6.91 A
S ₁	7.92 b	6.01 f	5.23 i	5.66 g	5.21 i	6.00 B
S ₂	6.90 d	5.39 hi	4.52 k	5.22 i	4.84 j	5.38 C
Mean	7.99 A	6.27 B	5.11 E	5.80 C	5.34 D	
	b (mg Ni kg ⁻¹) ⁻¹					
S ₀	0.196 i	0.222 g	0.247 d	0.238 e	0.237 e	0.228 C
S ₁	0.212 h	0.238 e	0.246 d	0.250 cd	0.254 bc	0.240 B
S ₂	0.230 f	0.254 bc	0.264 a	0.256 b	0.262 a	0.253 A
Mean	0.212 E	0.238 D	0.252 A	0.248 B	0.251 AB	
	ab					
S ₀	1.79 a	1.68 c	1.37 h	1.54 e	1.41 g	1.55 A
S ₁	1.69 b	1.43 f	1.29 k	1.41 fg	1.32 j	1.42 B
S ₂	1.59 d	1.37 h	1.19 m	1.34 i	1.27 l	1.35 C
Mean	1.69 A	1.48 B	1.28 E	1.43 C	1.33 D	

Notes: C, control; SM300, sheep manure biochar produced at 300 °C; SM500, sheep manure biochar produced at 500 °C; RH300, rice husk biochar produced at 300 °C; RH500, rice husk biochar produced at 500 °C; S₀, without Si addition; S₁, application of 250 mg Si kg⁻¹ soil; S₂, application of 500 mg Si kg⁻¹ soil.

516 * Numbers followed by same letters in each column and rows, in each section, are not significantly (P<0.05) different

517 The correlation between the parameters of the fitted power function model with soil Ni-
 518 chemical fractions, shoot Ni content and soil pH are shown in Table 8. The 'a' and 'ab' parameters
 519 had a positive correlation with the soil WsEx, OM and MnOx Ni fractions, while there was a
 520 negative correlation among the 'a' and 'ab' parameters the AFeOx and CFeOx Ni fractions. This
 521 trend was inverse for the 'b' parameter of the power function model. These correlations verified
 522 that the application of silicon and biochar to the Ni-contaminated calcareous soil led to a decrease
 523 in the rate and amount of Ni release from the soil by reducing the Ni concentration in chemical
 524 forms with higher bioavailability including WsEx, OM and MnOx. Furthermore, the 'a' and 'ab'
 525 parameters were negatively correlated with soil pH. Whereas there were positive correlations
 526 between these parameters and shoot Ni concentration (Table 8). These findings once again
 527 confirmed that the increase in soil pH due to the application of silicon and biochar can cause a
 528 decrease in the bioavailability of soil Ni and, as a result, a decrease in the concentration of Ni in
 529 aerial parts of the plant.

Table 8

The correlation coefficients (r) between the power function model parameters (a, b, ab) and soil Ni chemical fractions, shoot Ni concentration and soil pH.

	WsEx	Car	OM	MnOx	AFeOx	CFeOx	Res	Shoot Ni Concentration	Soil pH
a	0.63**	0.02 ^{ns}	0.70**	0.53**	-0.44**	-0.80**	0.27 ^{ns}	0.62**	-0.52**
b	-0.59**	0.03 ^{ns}	-0.68**	-0.54**	0.46**	0.83**	-0.28 ^{ns}	-0.63**	0.51**
ab	0.68**	0.04 ^{ns}	0.74**	0.46**	-0.46**	-0.80**	0.29 ^{ns}	0.06**	-0.51**

Notes: WsEx, water soluble and exchangeable fraction; OM, organic fraction; MnOx, bound to manganese oxides; AFeOx, bound to amorphous iron oxides; CFeOx, bound to crystalline iron oxides; Res, residual fraction.

** and ^{ns} indicate significance at the 0.01 probability level and non-significant, respectively.

530

531 **4 Conclusions**

532 The application of biochars and Si in the present study resulted in the transformation of Ni
533 in the soil from more bioavailable and mobile fractions (WsEx, MnOx, OM) to more stable forms
534 (AFeOx and CFeOx). These changes were particularly evident in the WsEx fraction when SM
535 biochars were applied in conjunction with silicon, indicating a strong synergistic effect related to
536 soil pH increase. Application of all biochars and Si reduced DPTA-extractable Ni release from the
537 soil, which was most strongly associated with the increase in CFeOx fraction. Application of all
538 biochars and Si decreased corn Ni uptake, with the combined SM500+S₂ being the most effective.
539 The decrease in corn uptake was correlated with the decrease in the WsEx-Ni fraction and increase
540 in CFeOx fraction. SM500 was likely the most effective biochar due to its higher alkalinity and
541 ash content, and lower acidic functional group content which enhanced Ni sorption reactions with
542 Si. Future research is needed to better understand the mechanisms underlying the interaction
543 effects of Si and biochar application on the distribution of soil Ni chemical forms and to optimize
544 Si application strategies for sustainable Ni management in agricultural and natural ecosystems.

545 **Authors' Contributions** H.R.B. Conceptualization, Formal analysis, Methodology, Investigation,
546 Validation A.G.H. Writing - Review & Editing M.N. Project administration, Visualization E.B.
547 Review & Editing E.F. Laboratory analyses.

548 **Financial support.** No funding was received for conducting this study.

549 **Competing interests.** The contact author has declared that neither they nor their co-authors have
550 any competing interests.

551 **Data availability.** The data generated in this study are available from the corresponding authors
552 upon reasonable request.

553 **Disclaimer.** Publisher's note: Copernicus Publications remains neutral with regard to
554 jurisdictional claims in published maps and institutional affiliations.

555 **Acknowledgements:** This work was supported by College of Agriculture and Natural Resources of Darab,
556 Shiraz University, Darab, Iran.

557 **References**

- 558 Abdelhafez, A. A., Li, J., and Abbas, M. H.: Feasibility of biochar manufactured from organic wastes on
559 the stabilization of heavy metals in a metal smelter contaminated soil, *Chemosphere*, 117, 66-71, 2014.
- 560 Adrees, M., Ali, S., Rizwan, M., Zia-ur-Rehman, M., Ibrahim, M., Abbas, F., Farid, M., Qayyum, M. F.,
561 and Irshad, M. K.: Mechanisms of silicon-mediated alleviation of heavy metal toxicity in plants: a
562 review, *Ecotoxicology and Environmental Safety*, 119, 186-197, 2015.
- 563 Ahmad, M., Rajapaksha, A. U., Lim, J. E., Zhang, M., Bolan, N., Mohan, D., Vithanage, M., Lee, S. S.,
564 and Ok, Y. S.: Biochar as a sorbent for contaminant management in soil and water: a review,
565 *Chemosphere*, 99, 19-33, 2014.
- 566 Alam, M. S., Gorman-Lewis, D., Chen, N., Flynn, S. L., Ok, Y. S., Konhauser, K. O., and Alessi, D. S.:
567 Thermodynamic analysis of nickel (II) and zinc (II) adsorption to biochar, *Environmental science &*
568 *technology*, 52, 6246-6255, 2018.
- 569 Anand, A., Gautam, S., and Ram, L. C.: Feedstock and pyrolysis conditions affect suitability of biochar for
570 various sustainable energy and environmental applications, *Journal of Analytical and Applied*
571 *Pyrolysis*, 170, 105881, 2023.

- 572 Ankita Rao, K., Nair, V., Divyashri, G., Krishna Murthy, T., Dey, P., Samrat, K., Chandraprabha, M., and
573 Hari Krishna, R.: Role of Lignocellulosic Waste in Biochar Production for Adsorptive Removal of
574 Pollutants from Wastewater, in: *Advanced and Innovative Approaches of Environmental*
575 *Biotechnology in Industrial Wastewater Treatment*, Springer, 221-238, 2023.
- 576 Antoniadis, V., Levizou, E., Shaheen, S. M., Ok, Y. S., Sebastian, A., Baum, C., Prasad, M. N., Wenzel,
577 W. W., and Rinklebe, J.: Trace elements in the soil-plant interface: Phytoavailability, translocation,
578 and phytoremediation—A review, *Earth-Science Reviews*, 171, 621-645, 2017.
- 579 Bandara, T., Franks, A., Xu, J., Bolan, N., Wang, H., and Tang, C.: Chemical and biological immobilization
580 mechanisms of potentially toxic elements in biochar-amended soils, *Critical Reviews in*
581 *Environmental Science and Technology*, 50, 903-978, 2020.
- 582 Belton, D. J., Deschaume, O., and Perry, C. C.: An overview of the fundamentals of the chemistry of silica
583 with relevance to biosilicification and technological advances, *The FEBS journal*, 279, 1710-1720,
584 2012.
- 585 Bharti, K. P., Pradhan, A. K., Singh, M., Beura, K., Behera, S. K., and Paul, S. C.: Effect of mycorrhizal
586 co-Inoculation with selected rhizobacteria on soil zinc dynamics, *International Journal of Current*
587 *Microbiology and Applied Sciences*, 7, 1961-1970, 2018.
- 588 Bhat, J. A., Shivraj, S., Singh, P., Navadagi, D. B., Tripathi, D. K., Dash, P. K., Solanke, A. U., Sonah,
589 H., and Deshmukh, R.: Role of silicon in mitigation of heavy metal stresses in crop plants, *Plants*, 8,
590 71, 2019.
- 591 Boostani, H., Hardie, A., Najafi-Ghiri, M., and Khalili, D.: Investigation of cadmium immobilization in a
592 contaminated calcareous soil as influenced by biochars and natural zeolite application, *International*
593 *journal of environmental science and technology*, 15, 2433-2446, 2018a.
- 594 Boostani, H., Hardie, A., Najafi-Ghiri, M., and Khalili, D.: Investigation of cadmium immobilization in a
595 contaminated calcareous soil as influenced by biochars and natural zeolite application, *International*
596 *Journal of Environmental Science and Technology*, 15, 2433-2446, 2018b.
- 597 Boostani, H. R., Hardie, A. G., and Najafi-Ghiri, M.: Chemical fractions, mobility and release kinetics of
598 Cadmium in a light-textured calcareous soil as affected by crop residue biochars and Cd-contamination
599 levels, *Chemistry and Ecology*, 1-14, 2023a.
- 600 Boostani, H. R., HARDIE, A. G., and NAJAFI-GHIRI, M.: Lead stabilization in a polluted calcareous soil
601 using cost-effective biochar and zeolite amendments after spinach cultivation, *Pedosphere*, 33, 321-
602 330, 2023b.
- 603 Boostani, H. R., Najafi-Ghiri, M., and Mirsoleimani, A.: The effect of biochars application on reducing the
604 toxic effects of nickel and growth indices of spinach (*Spinacia oleracea* L.) in a calcareous soil,
605 *Environmental Science and Pollution Research*, 26, 1751-1760, 2019a.
- 606 Boostani, H. R., Hardie, A. G., Najafi-Ghiri, M., and Khalili, D.: The effect of soil moisture regime and
607 biochar application on lead (Pb) stabilization in a contaminated soil, *Ecotoxicology and Environmental*
608 *Safety*, 208, 111626, 2021.
- 609 Boostani, H. R., Hardie, A. G., Najafi-Ghiri, M., and Zare, M.: Chemical speciation and release kinetics of
610 Ni in a Ni-contaminated calcareous soil as affected by organic waste biochars and soil moisture regime,
611 *Environmental Geochemistry and Health*, 45, 199-213, 2023c.
- 612 Boostani, H. R., Najafi-Ghiri, M., Amin, H., and Mirsoleimani, A.: Zinc desorption kinetics from some
613 calcareous soils of orange (*Citrus sinensis* L.) orchards, southern Iran, *Soil science and plant nutrition*,
614 65, 20-27, 2019b.
- 615 Chatterjee, R., Sajjadi, B., Chen, W.-Y., Mattern, D. L., Hammer, N., Raman, V., and Dorris, A.: Effect of
616 pyrolysis temperature on physicochemical properties and acoustic-based amination of biochar for
617 efficient CO₂ adsorption, *Frontiers in Energy Research*, 8, 85, 2020.
- 618 Claoston, N., Samsuri, A., Ahmad Husni, M., and Mohd Amran, M.: Effects of pyrolysis temperature on
619 the physicochemical properties of empty fruit bunch and rice husk biochars, *Waste Management &*
620 *Research*, 32, 331-339, 2014.
- 621 Dalal, R.: Comparative prediction of yield response and phosphorus uptake from soil using anion-and
622 cation-anion-exchange resins, *Soil Science*, 139, 227-231, 1985.

623 Dang, Y., Dalal, R., Edwards, D., and Tiller, K.: Kinetics of zinc desorption from Vertisols, Soil Science
624 Society of America Journal, 58, 1392-1399, 1994.

625 Deng, Y., Huang, S., Laird, D. A., Wang, X., and Meng, Z.: Adsorption behaviour and mechanisms of
626 cadmium and nickel on rice straw biochars in single-and binary-metal systems, Chemosphere, 218,
627 308-318, 2019.

628 Derakhshan Nejad, Z., Jung, M. C., and Kim, K.-H.: Remediation of soils contaminated with heavy metals
629 with an emphasis on immobilization technology, Environmental geochemistry and health, 40, 927-
630 953, 2018.

631 Dey, D., Sarangi, D., and Mondal, P.: Biochar: Porous Carbon Material, Its Role to Maintain Sustainable
632 Environment, in: Handbook of Porous Carbon Materials, Springer, 595-621, 2023.

633 El-Naggar, A., Rajapaksha, A. U., Shaheen, S. M., Rinklebe, J., and Ok, Y. S.: Potential of biochar to
634 immobilize nickel in contaminated soils, in: Nickel in Soils and Plants, CRC Press, 293-318, 2018.

635 El-Naggar, A., Chang, S. X., Cai, Y., Lee, Y. H., Wang, J., Wang, S.-L., Ryu, C., Rinklebe, J., and Ok, Y.
636 S.: Mechanistic insights into the (im) mobilization of arsenic, cadmium, lead, and zinc in a multi-
637 contaminated soil treated with different biochars, Environment International, 156, 106638, 2021.

638 Gao, W., He, W., Zhang, J., Chen, Y., Zhang, Z., Yang, Y., and He, Z.: Effects of biochar-based materials
639 on nickel adsorption and bioavailability in soil, Scientific Reports, 13, 5880, 2023.

640 Gee, G. W. and Bauder, J. W.: Particle-size analysis, Methods of soil analysis: Part 1 Physical and
641 mineralogical methods, 5, 383-411, 1986.

642 Ghasemi-Fasaei, R., Maftoun, M., Ronaghi, A., Karimian, N., Yasrebi, J., Assad, M., and Ippolito, J.:
643 Kinetics of copper desorption from highly calcareous soils, Communications in Soil Science and Plant
644 Analysis, 37, 797-809, 2006.

645 Ghiri, M. N., Abtahi, A., Owliaie, H., Hashemi, S. S., and Koohkan, H.: Factors affecting potassium pools
646 distribution in calcareous soils of southern Iran, Arid land research and management, 25, 313-327,
647 2011.

648 Hossain, M. A., Piyatida, P., da Silva, J. A. T., and Fujita, M.: Molecular mechanism of heavy metal toxicity
649 and tolerance in plants: central role of glutathione in detoxification of reactive oxygen species and
650 methylglyoxal and in heavy metal chelation, Journal of botany, 2012, 2012.

651 Ippolito, J., Berry, C., Strawn, D., Novak, J., Levine, J., and Harley, A.: Biochars reduce mine land soil
652 bioavailable metals, Journal of environmental quality, 46, 411-419, 2017.

653 Kamali, S., Ronaghi, A., and Karimian, N.: Soil zinc transformations as affected by applied zinc and organic
654 materials, Communications in soil science and plant analysis, 42, 1038-1049, 2011.

655 Kameyama, K., Miyamoto, T., and Iwata, Y.: The preliminary study of water-retention related properties
656 of biochar produced from various feedstock at different pyrolysis temperatures, Materials, 12, 1732,
657 2019.

658 Kandpal, G., Srivastava, P., and Ram, B.: Kinetics of desorption of heavy metals from polluted soils:
659 Influence of soil type and metal source, Water, Air, and Soil Pollution, 161, 353-363, 2005.

660 Keiluweit, M., Nico, P. S., Johnson, M. G., and Kleber, M.: Dynamic molecular structure of plant biomass-
661 derived black carbon (biochar), Environmental science & technology, 44, 1247-1253, 2010.

662 Khaliq, A., Ali, S., Hameed, A., Farooq, M. A., Farid, M., Shakoor, M. B., Mahmood, K., Ishaque, W., and
663 Rizwan, M.: Silicon alleviates nickel toxicity in cotton seedlings through enhancing growth,
664 photosynthesis, and suppressing Ni uptake and oxidative stress, Archives of Agronomy and Soil
665 Science, 62, 633-647, 2016.

666 Li, X.: Technical solutions for the safe utilization of heavy metal-contaminated farmland in China: a critical
667 review, Land Degradation & Development, 30, 1773-1784, 2019.

668 Liang, Y., Wong, J., and Wei, L.: Silicon-mediated enhancement of cadmium tolerance in maize (*Zea mays*
669 L.) grown in cadmium contaminated soil, Chemosphere, 58, 475-483, 2005.

670 Lindsay, W. L. and Norvell, W.: Development of a DTPA soil test for zinc, iron, manganese, and copper,
671 Soil science society of America journal, 42, 421-428, 1978.

672 Liu, L., Guo, X., Wang, S., Li, L., Zeng, Y., and Liu, G.: Effects of wood vinegar on properties and
673 mechanism of heavy metal competitive adsorption on secondary fermentation based composts,
674 *Ecotoxicology and environmental safety*, 150, 270-279, 2018.

675 Loeppert, R. H. and Suarez, D. L.: Carbonate and gypsum, *Methods of soil analysis: Part 3 chemical*
676 *methods*, 5, 437-474, 1996.

677 Lu, K., Yang, X., Gielen, G., Bolan, N., Ok, Y. S., Niazi, N. K., Xu, S., Yuan, G., Chen, X., and Zhang,
678 X.: Effect of bamboo and rice straw biochars on the mobility and redistribution of heavy metals (Cd,
679 Cu, Pb and Zn) in contaminated soil, *Journal of environmental management*, 186, 285-292, 2017.

680 Ma, C., Ci, K., Zhu, J., Sun, Z., Liu, Z., Li, X., Zhu, Y., Tang, C., Wang, P., and Liu, Z.: Impacts of
681 exogenous mineral silicon on cadmium migration and transformation in the soil-rice system and on
682 soil health, *Science of the Total Environment*, 759, 143501, 2021.

683 Mailakeba, C. D. and BK, R. R.: Biochar application alters soil Ni fractions and phytotoxicity of Ni to
684 pakchoi (*Brassica rapa L. ssp. chinensis L.*) plants, *Environmental Technology & Innovation*, 23,
685 101751, 2021.

686 Maruyama, M., Sawada, K. P., Tanaka, Y., Okada, A., Momma, K., Nakamura, M., Mori, R., Furukawa,
687 Y., Sugiura, Y., and Tajiri, R.: Quantitative analysis of calcium oxalate monohydrate and dihydrate
688 for elucidating the formation mechanism of calcium oxalate kidney stones, *Plos one*, 18, e0282743,
689 2023.

690 Maryam, H., Abbasi, G. H., Waseem, M., Ahmed, T., and Rizwan, M.: Preparation and characterization of
691 green silicon nanoparticles and their effects on growth and lead (Pb) accumulation in maize (*Zea mays*
692 *L.*), *Environmental Pollution*, 123691, 2024.

693 Myszka, B., Schüßler, M., Hurle, K., Demmert, B., Detsch, R., Boccaccini, A. R., and Wolf, S. E.: Phase-
694 specific bioactivity and altered Ostwald ripening pathways of calcium carbonate polymorphs in
695 simulated body fluid, *RSC advances*, 9, 18232-18244, 2019.

696 Nasrabadi, M., Omid, M. H., and Mazdeh, A. M.: Experimental Study of Flow Turbulence Effect on
697 Cadmium Desorption Kinetics from Riverbed Sands, *Environmental Processes*, 9, 10, 2022.

698 Nelson, D. W. and Sommers, L. E.: Total carbon, organic carbon, and organic matter, *Methods of soil*
699 *analysis: Part 3 Chemical methods*, 5, 961-1010, 1996.

700 Okolo, C. C., Gebresamuel, G., Zenebe, A., Haile, M., Orji, J. E., Okebalama, C. B., Eze, C. E., Eze, E.,
701 and Eze, P. N.: Soil organic carbon, total nitrogen stocks and CO₂ emissions in top-and subsoils with
702 contrasting management regimes in semi-arid environments, *Scientific Reports*, 13, 1117, 2023.

703 Poznanović Spahić, M. M., Sakan, S. M., Glavaš-Trbić, B. M., Tančić, P. I., Škrivanj, S. B., Kovačević, J.
704 R., and Manojlović, D. D.: Natural and anthropogenic sources of chromium, nickel and cobalt in soils
705 impacted by agricultural and industrial activity (Vojvodina, Serbia), *Journal of Environmental Science*
706 *and Health, Part A*, 54, 219-230, 2019.

707 Rhoades, J.: Salinity: Electrical conductivity and total dissolved solids, *Methods of soil analysis: Part 3*
708 *Chemical methods*, 5, 417-435, 1996.

709 Rizwan, M., Ali, S., Qayyum, M. F., Ibrahim, M., Zia-ur-Rehman, M., Abbas, T., and Ok, Y. S.:
710 Mechanisms of biochar-mediated alleviation of toxicity of trace elements in plants: a critical review,
711 *Environmental Science and Pollution Research*, 23, 2230-2248, 2016.

712 Sachdeva, S., Kumar, R., Sahoo, P. K., and Nadda, A. K.: Recent advances in biochar amendments for
713 immobilization of heavy metals in an agricultural ecosystem: A systematic review, *Environmental*
714 *Pollution*, 319, 120937, 2023.

715 Saffari, M., Karimian, N., Ronaghi, A., Yasrebi, J., and Ghasemi-Fasaei, R.: Stabilization of nickel in a
716 contaminated calcareous soil amended with low-cost amendments, *Journal of soil science and plant*
717 *nutrition*, 15, 896-913, 2015.

718 Sajadi Tabar, S. and Jalali, M.: Kinetics of Cd release from some contaminated calcareous soils, *Natural*
719 *resources research*, 22, 37-44, 2013.

720 Shahbazi, K., Fathi-Gerdelidani, A., and Marzi, M.: Investigation of the status of heavy metals in soils of
721 Iran: A comprehensive and critical review of reported studies, *Iranian Journal of Soil and Water*
722 *Research*, 53, 1163-1212, 10.22059/ijswr.2022.341586.669245, 2022.

723 Shahbazi, K., Marzi, M., and Rezaei, H.: Heavy metal concentration in the agricultural soils under the
724 different climatic regions: a case study of Iran, *Environmental earth sciences*, 79, 324, 2020.

725 Shahzad, B., Tanveer, M., Rehman, A., Cheema, S. A., Fahad, S., Rehman, S., and Sharma, A.: Nickel;
726 whether toxic or essential for plants and environment-A review, *Plant Physiology and Biochemistry*,
727 132, 641-651, 2018.

728 Shen, B., Wang, X., Zhang, Y., Zhang, M., Wang, K., Xie, P., and Ji, H.: The optimum pH and Eh for
729 simultaneously minimizing bioavailable cadmium and arsenic contents in soils under the organic
730 fertilizer application, *Science of the Total Environment*, 711, 135229, 2020.

731 Singh, J., Karwasra, S., and Singh, M.: Distribution and forms of copper, iron, manganese, and zinc in
732 calcareous soils of India, *Soil Science*, 146, 359-366, 1988.

733 Sparks, D. L., Singh, B., and Siebecker, M. G.: *Environmental soil chemistry*, Elsevier2022.

734 Sparrow, L. and Uren, N.: Manganese oxidation and reduction in soils: effects of temperature, water
735 potential, pH and their interactions, *Soil Research*, 52, 483-494, 2014.

736 Sumner, M. E. and Miller, W. P.: Cation exchange capacity and exchange coefficients, *Methods of soil
737 analysis: Part 3 Chemical methods*, 5, 1201-1229, 1996.

738 Sun, L., Zhang, G., Li, X., Zhang, X., Hang, W., Tang, M., and Gao, Y.: Effects of biochar on the
739 transformation of cadmium fractions in alkaline soil, *Heliyon*, e12949, 2023.

740 Sun, Y., Gao, B., Yao, Y., Fang, J., Zhang, M., Zhou, Y., Chen, H., and Yang, L.: Effects of feedstock type,
741 production method, and pyrolysis temperature on biochar and hydrochar properties, *Chemical
742 engineering journal*, 240, 574-578, 2014.

743 Tomczyk, A., Sokołowska, Z., and Boguta, P.: Biochar physicochemical properties: pyrolysis temperature
744 and feedstock kind effects, *Reviews in Environmental Science and Bio/Technology*, 19, 191-215,
745 2020.

746 Uchimiya, M., Lima, I. M., Thomas Klasson, K., Chang, S., Wartelle, L. H., and Rodgers, J. E.:
747 Immobilization of heavy metal ions (CuII, CdII, NiII, and PbII) by broiler litter-derived biochars in
748 water and soil, *Journal of agricultural and food chemistry*, 58, 5538-5544, 2010.

749 Vickers, N. J.: Animal communication: when i'm calling you, will you answer too?, *Current biology*, 27,
750 R713-R715, 2017.

751 Xiao, Z., Peng, M., Mei, Y., Tan, L., and Liang, Y.: Effect of organosilicone and mineral silicon fertilizers
752 on chemical forms of cadmium and lead in soil and their accumulation in rice, *Environmental
753 Pollution*, 283, 117107, 2021.

754 Yan, G.-c., Nikolic, M., YE, M.-j., Xiao, Z.-x., and LIANG, Y.-c.: Silicon acquisition and accumulation in
755 plant and its significance for agriculture, *Journal of Integrative Agriculture*, 17, 2138-2150, 2018.

756 Yuan, J.-H., Xu, R.-K., and Zhang, H.: The forms of alkalis in the biochar produced from crop residues at
757 different temperatures, *Bioresource technology*, 102, 3488-3497, 2011.

758 Zemnukhova, L. A., Panasenko, A. E., Artem'yanov, A. P., and Tsoy, E. A.: Dependence of porosity of
759 amorphous silicon dioxide prepared from rice straw on plant variety, *BioResources*, 10, 3713-3723,
760 2015.

761 Zeng, X., Xiao, Z., Zhang, G., Wang, A., Li, Z., Liu, Y., Wang, H., Zeng, Q., Liang, Y., and Zou, D.:
762 Speciation and bioavailability of heavy metals in pyrolytic biochar of swine and goat manures, *Journal
763 of Analytical and Applied Pyrolysis*, 132, 82-93, 2018.

764 Zhao, S.-X., Ta, N., and Wang, X.-D.: Effect of temperature on the structural and physicochemical
765 properties of biochar with apple tree branches as feedstock material, *Energies*, 10, 1293, 2017.

766 Zhu, Q., Wu, J., Wang, L., Yang, G., and Zhang, X.: Effect of biochar on heavy metal speciation of paddy
767 soil, *Water, Air, & Soil Pollution*, 226, 1-10, 2015.

768